

# Pitch Angle Scattering by Electromagnetic Ion Cyclotron Triggered Emissions in the Inner Magnetosphere: Hybrid Simulations

*Masafumi Shoji<sup>1</sup>, Yoshiharu Omura<sup>1</sup>*

<sup>1</sup>Research Institute for Sustainable Humanosphere, Kyoto University, Gokasho, Uji, Kyoto, Japan, shouji@rish.kyoto-u.ac.jp, omura@rish.kyoto-u.ac.jp

## Abstract

In a recent observation by the Cluster spacecraft, electromagnetic ion cyclotron (EMIC) triggered emissions were discovered in the inner magnetosphere. We perform hybrid simulations to reproduce the EMIC triggered emissions. We develop a self-consistent one-dimensional (1D) hybrid code with a cylindrical geometry of the background magnetic field. We assume a parabolic magnetic field to model the dipole magnetic field in the equatorial region of the inner magnetosphere. Triggering EMIC waves are driven by a left-handed polarized external current assumed at the magnetic equator in the simulation model. Cold proton, helium, and oxygen ions, which form branches of the dispersion relation of the EMIC waves, are uniformly distributed in the simulation space. Energetic protons with a loss cone distribution function are also assumed as resonant particles. We reproduce rising tone emissions in the simulation space, finding a good agreement with the nonlinear wave growth theory. In the energetic proton velocity distribution we find formation of a proton hole, which is assumed in the nonlinear wave growth theory. A substantial amount of the energetic protons are scattered into the loss cone, while some of the resonant protons are accelerated to higher pitch angles, forming a pancake velocity distribution.

## 1. Introduction

Recent Cluster observations around the equatorial region of the Earth's inner magnetosphere discovered coherent ULF rising-tone emissions [1] whose frequency characteristics are very similar to those of whistler-mode VLF chorus emissions [2], [3]. These ULF emissions arise from almost constant frequency waves lower than the proton cyclotron frequency  $\sim 3.7$  Hz. The observation result indicates that these rising-tone emissions always need the EMIC waves as triggering waves. These chorus-like ULF emissions are called EMIC triggered emissions [1], [4], [5]. A nonlinear wave growth theory explaining the EMIC triggered emissions have been developed [4]. The theory has a good agreement with observations in the frequency sweep rate of the rising-tone emissions. The saturation mechanism of the wave growth, however, has not been explained by the theory yet. To understand the nonlinear processes including the saturation and associated acceleration or pitch angle scattering of energetic protons, we need to analyze the time evolution of the interaction between the EMIC triggered emissions and the energetic protons quantitatively. In the present study [5], we reproduce the generation process of the EMIC triggered emissions by a self-consistent hybrid code with a parabolic magnetic field. We perform a hybrid simulation with realistic parameters around the magnetic equator at  $L \sim 4.3$ , and compare the results with the observations and theory.

One dimensional (1D) hybrid code along  $x$  direction is developed [5]. While the field equations are solved as the 1D system taken along the  $x$  axis, the background magnetic field has a cylindrical geometry around the  $x$  axis, and ions are assumed to gyrate around the magnetic field with finite cyclotron radii. The  $x$  component of the background magnetic field is defined by a parabolic function as an approximation of the dipole magnetic field of the Earth at  $L \sim 4.3$ . Three kinds of cold ions ( $H^+$ ,  $He^+$ , and  $O^+$ ), and energetic protons are assumed in the simulation. Realistic parameters for the ions and the triggering wave which is driven by the left-polarized external current at the equator ( $x=0$ ) are assumed.

## 2. Simulation of the EMIC triggered emissions

### 2.1 Comparison with the nonlinear theory and the observations

A Fourier transform in a limited time window is applied for electric fields of both forward and backward propagating waves at the equatorial region. Sliding the window from the initial time to the end of the simulation period, we obtain the time evolution of the wave spectra. The size of the window is taken as  $t \sim 11.2$  s for a sufficient resolution

in the frequency domain. Figure 1 show dynamic spectra of the electric field the forward and backward propagating waves around the equatorial region obtained by this method, respectively. The EMIC triggered emissions are successfully reproduced both in the forward and backward propagating waves. The duration of the rising tone emissions from 1.5 Hz to 3.0 Hz is 45 s in this case, showing a good agreement with the observation [1] and the theory [4]. The frequency predicted by the theory is shown by the white lines in Figure 1. We find a good agreement with the theory in the initial phase of the triggered emissions. Because this theory does not include the saturation mechanism, the theoretical frequency becomes different from that of the simulation result after  $\sim 40$  s.

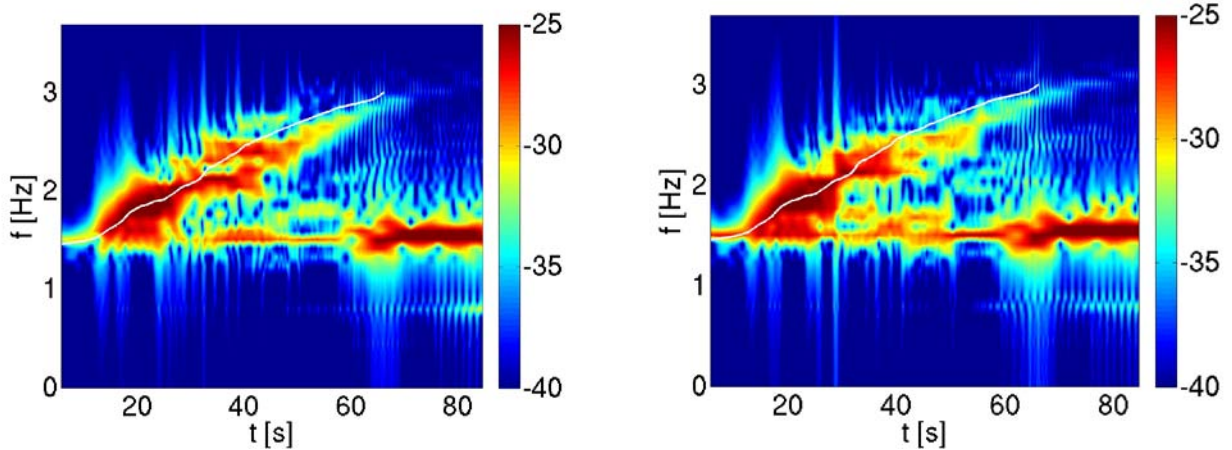


Figure 1: Dynamic spectra of the electric field of forward (left) and backward (right) waves. The white lines indicate the theoretical time evolution of the frequency of the EMIC triggered emissions.

## 2.2. Pitch angle scattering and particle acceleration

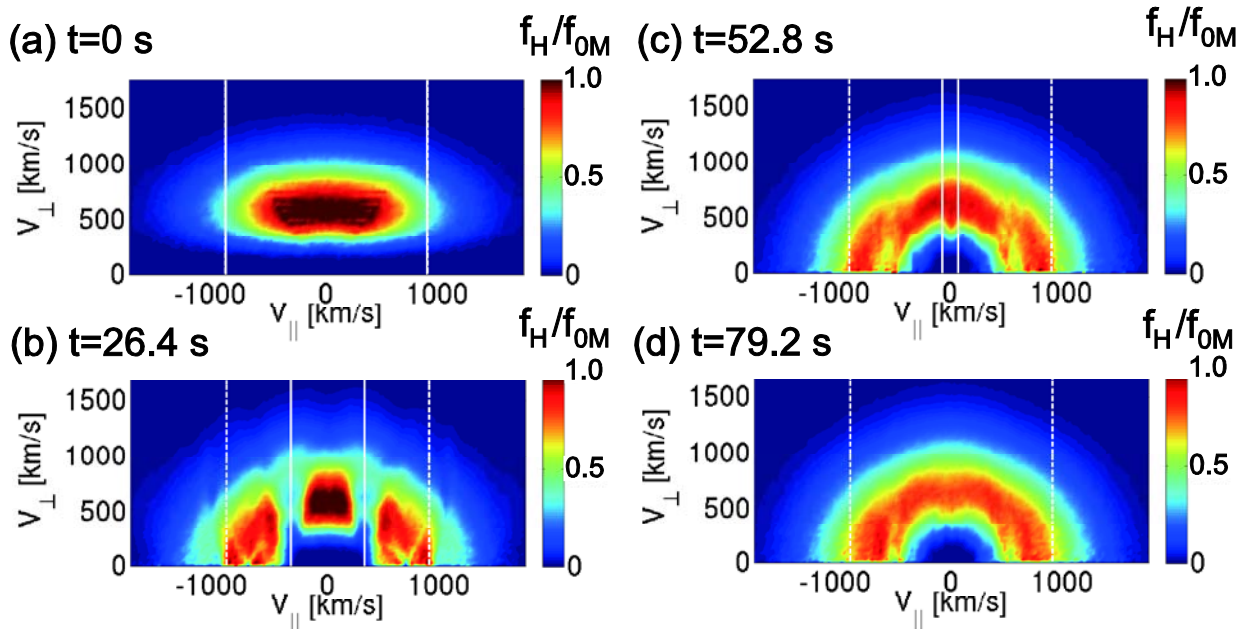
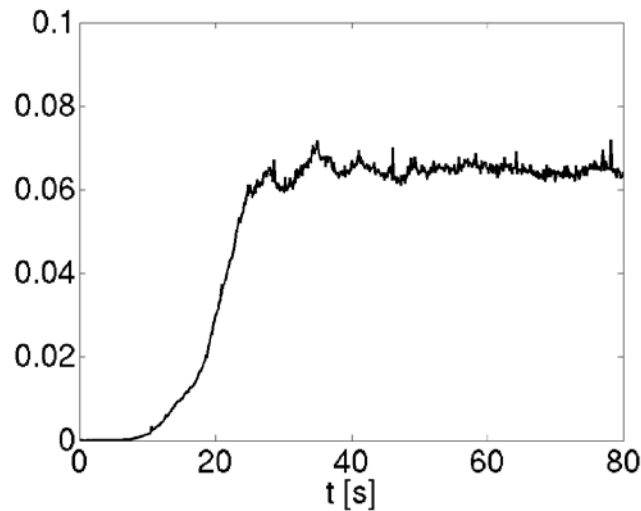


Figure 2: Time evolution of the velocity distribution function of the energetic protons around the equator at (a)  $t=0$  s, (b)  $t=26.4$  s, (c)  $t=52.8$  s, and (d)  $t=79.2$  s [5]. The white solid and dashed lines show the resonance velocity of the triggered and triggering waves, respectively.

The velocity distribution functions of energetic protons around the equatorial region at different times are shown in Figure 2 [5]. The values of the velocity distribution functions are normalized by the maximum value of the initial velocity distribution function  $f_{0M}$ . We show these panels at equal time intervals of 26.4 s. The white solid lines indicate the resonance velocities of the forward ( $k>0$ ) and backward ( $k<0$ ) propagating triggered waves. We also show the resonance velocities of the forward and backward triggering waves by white dashed lines. The initial distribution function is shown in Figure 2a. As the EMIC triggered emissions evolve in time, the resonant velocities become smaller in magnitude because of the increasing frequencies and wavenumbers. Thus the energetic protons with smaller parallel velocities are strongly scattered as shown in Figures 2b, 2c, and 2d. At  $t=26.4$  s (shown in Figure 2b) the triggered waves saturate, we can find proton holes around the resonance velocities of the triggered wave. Energetic protons around the resonance velocity are strongly scattered in their pitch angles. As we find in Figure 2c, the proton holes are gradually filled out by the scattered resonant protons. The frequencies of the triggered waves still increase and thus the core part of the distribution function of the energetic protons is diffused. Finally, as shown in Figure 2d after the triggered waves saturate and disappear, the distribution function becomes stable. At this time, the whole core of the initial distribution disappears. A substantial number of the energetic protons in a wide range of energy are scattered through the generation process of the triggered emissions. Thus the distribution of the energetic protons shows a very different distribution from the initial one, indicating strong pitch angle scattering by the triggered emissions over one cycle of the nonlinear triggering process.

Comparing between Figures 2a and 2d, we can also find increase of energetic protons around pitch angles  $\sim 90$  degree. We integrate the increased density of the energetic protons which have  $V_{\perp}>900$  km/s. During the generation process of the triggered emissions, nearly 2.4 % of energetic protons in the equatorial region are accelerated. The acceleration is due to phase trapping of resonant protons guided from the upstream regions toward the equator along the resonance velocity, which decreases to the lower value in magnitude. Because of the energy transfer from the waves to the accelerated protons, the nonlinear wave growth near the equator is saturated, and triggered waves are subsequently damped.



**Figure 3: Time evolution of the amount of energetic protons in the loss cone around the equatorial regions.**

As we find in Figure 2, Most of the energetic protons are scattered and some of them are fall into the loss cone. These precipitating particles can cause the proton aurora in the polar region. Figure 3 shows the time evolution of the amount of the energetic protons which have the pitch angle smaller than the loss cone angle 4.8 degree at  $L=4.3$  at the equator. The value is normalized by the number of the total energetic protons around the equatorial region. The number of precipitating protons saturate around  $t \sim 20$  s. This time corresponds to the saturation time of the EMIC triggered emission [5] and the number does not change after the saturation. Thus, the most of the precipitation is caused before the saturation of the triggered emission. At  $t=79.2$  s, after the triggered emission disappears, 6.8 % of the energetic protons become in the loss cone and they have the energy around 4.5 keV.

## 4. Summary

- We have developed a 1D hybrid code with a cylindrical magnetic field model to analyze the nonlinear wave growth of EMIC triggered emissions in dipole geometry, reproducing the rising-tone emissions from injected EMIC triggering waves around the equatorial region with realistic parameters. The duration and the frequency sweep rate of the triggered emissions show a good agreement with observations and nonlinear wave growth theory.
- The proton velocity distribution is strongly modulated by formation of large proton holes due to the triggered emissions. The rising tone emissions drive the proton holes to a lower parallel velocity because of the decreasing resonance velocities.
- A substantial amount of energetic protons as large as 6.5% of the trapped protons are scattered into the loss cone in 45 s during which the triggered emissions are generated inside the plasmopause. These particles move away from the equator along the ambient magnetic field, and precipitate into the atmosphere, resulting in the proton aurora in the polar regions.

## 5. Acknowledgments

Computation in the present study was performed with the KDK system of Research Institute for Sustainable Humanosphere and Academic Center for Computing and Media Studies at Kyoto University as a collaborative research project. The present study was supported in part by Grant-in-Aid for Research Fellows from the Japan Society for the Promotion of Science, and Grant-in-Aid 20340135 of the Ministry of Education, Science, Sports and Culture of Japan.

## 6. References

1. Pickett, J. S., B. Grison, Y. Omura, M. J. Engebretson, I. Dandouras, A. Masson, M. L. Adrian, O. Santolik, P. M. E. Decreau, N. Cornilleau-Wehrin, and D. Constantinescu (2010), Cluster observations of EMIC triggered emissions in association with Pc1 waves near Earth's plasmopause, *Geophys. Res. Lett.*, *37*, L09104.
2. Omura, Y., Y. Katoh, and D. Summers (2008), Theory and simulation of the generation of whistler-mode chorus, *J. Geophys. Res.*, *113*, A04223.
3. Santolik, O., D. A. Gurnett, J. S. Pickett, M. Parrot, and N. Cornilleau - Wehrin (2003b), Spatio - temporal structure of storm - time chorus, *J. Geophys. Res.*, *108*(A7), 1278.
4. Omura, Y., J. Pickett, B. Grison, O. Santolik, I. Dandouras, M. Engebretson, P. M. E Decreau, and A. Masson (2010), Theory and observation of electromagnetic ion cyclotron chorus emissions in the magnetosphere, *J. Geophys. Res.*, *115*, A07234.
5. Shoji, M. and Y. Omura., Simulation of electromagnetic ion cyclotron triggered emissions in the magnetosphere, *J. Geophys. Res.*, *in press*.